# Isotope Exchange Technique for Measurement of Gas Adsorption Equilibria and Kinetics

**R. M. Rynders, M. B. Rao, and S. Sircar**
Air Products and Chemicals, Inc., Allentown, PA 18195

*The isotope exchange technique (IET) can be used to simultaneously measure multicomponent gas adsorption equilibria and self-diffusivities of the components in a single isothermal experiment without disturbing the overall adsorbed phase. An experimental protocol for the IET and corresponding data analysis procedures is described. Isotherms and self-diffusivities for adsorption of $N_2$ as a pure gas were measured on commercial samples of a carbon molecular sieve and a 4-Å zeolite using IET, as well as those of $O_2$ and $N_2$ from their binary mixtures. The carbon molecular sieve did not exhibit thermodynamic selectivity for air separation, but had a kinetic selectivity of $O_2$ over $N_2$. Mass-transfer resistances for self-diffusion of $N_2$ and $O_2$ on the carbon molecular sieve were controlled by pore mouth restrictions in the carbon, but those for adsorption of $N_2$ into the 4-Å zeolite by Fickian diffusion inside the adsorbent. A linear driving force model described the uptakes of $N_2$ and $O_2$ in the carbon molecular sieve. The Fickian diffusion model described the $N_2$ uptake in the 4-Å zeolite. Mass-transfer coefficients for both $O_2$ and $N_2$ on the carbon molecular sieve increased linearly with increasing gas-phase partial pressure of these gases, and the pressure of $O_2$ did not affect mass-transfer coefficients for $N_2$. The self-diffusivity of $N_2$ in the 4-Å zeolite decreased with increasing adsorbate loading.*

## Introduction

Accurate pure and multicomponent gas adsorption equilibria, isosteric heats, and kinetics are three key input variables for design and optimization of pressure swing adsorption (PSA) and thermal swing adsorption (TSA) processes for separation and purification of gaseous mixtures (Sircar, 1991; Hartzog and Sircar, 1995). Problems associated with determining these variables by conventional methods are discussed below.

### *Adsorption equilibria*

A large volume of experimental data on pure and binary gas adsorption equilibria is available in the published literature. Some of these data are compiled and systematically analyzed (Valenzuela and Myers, 1984, 1989). On the other hand, multicomponent (more than two components) adsorption equilibrium data are very sporadic despite the fact that most practical adsorptive separation processes involve multicomponent feed gas mixtures. There are three key reasons for this:

(a) The extent of data required to completely describe the multicomponent adsorption systems can be very large. Thus, the experimental process can be very tedious and time consuming. The Gibbsian surface excess (Sircar, 1985, 1996) of each component $i$ of the multicomponent system $[n_i^m,\ i = 1, 2, \ldots]$ must be measured as functions of total gas pressure ($P$), gas-phase mole fraction of component $i$ ($y_i$), and system temperature ($T$) in the entire range of these variables experienced by the adsorber during the PSA or TSA process steps.

(b) The most frequently used experimental methods to measure multicomponent gas ($i \geq 2$) adsorption equilibria such as the volumetric adsorption technique (VAT) and the total desorption technique (TDT) are not very convenient.

The VAT (Ross and Olivier, 1964) consists of contacting a known quantity of a gas mixture of known pressure and composition with an adsorbent mass and measuring the final equilibrium gas-phase pressure ($P$) and composition ($y_i$) of the system. The system temperature ($T$) is constant before

Correspondence concerning this article should be addressed to S. Sircar.

and after the equilibrium process. A mass balance of each component of the system then allows the calculation of $n_i^m$ (specific surface excess of component $i$) as functions of $P$, $T$ and $y_i$. There is, however, no control over the final equilibrium pressure and composition variables by this method and the data generated can be very random and impractical.

The TDT (Basmadjian, 1960; Kumar and Sircar, 1986) consists of saturating an adsorbent mass (kept in a thermostated container of known void volume) with a multicomponent gas mixture at a given condition ($P$, $T$, $y_i$), followed by complete removal of all components from the adsorption system by heating the adsorbent to its regeneration temperature and simultaneously evacuating the system. The quantity and composition of the desorbed and void gases are measured. A mass balance of each component allows the calculation of $n_i^m$ as functions of $P$, $T$, and $y_i$. Thus, the TDT gives complete control over the condition of measurement of equilibrium ($n_i^m$) but the method is rather laborious.

(c) Neither VAT or TDT are very convenient for checking the replicability of the measured multicomponent equilibrium data.

### *Isosteric heats*

The isoteric heats of adsorption of a pure gas $i$ ($q_i^0$) can be easily calculated as functions of its surface excess ($n_i^{mo}$) from a set of pure gas adsorption isotherms ($n_{io}^m$ vs. $P$ at different $T$) using a well-known thermodynamic relationship (Sircar, 1985). Such thermodynamic calculations of the component isosteric heats ($q_i$) of a multicomponent gas mixture ($i \geq 2$) as functions of the component surface excesses ($n_i^m$), on the other hand, require an extensive database covering multicomponent isotherms ($n_i^m$ vs. $P$ at constant $y_i$ and $T$), isobars ($n_i^m$ vs. $y_i$ at constant $P$ and $T$), and partial pressure isobars ($n_i^m$ vs. $T$ at constant $P$ and $y_i$) which are rarely available (Sircar, 1995). Compilation of such massive data may also be impractical.

Direct measurement of $q_i$ as functions of $n_i^m$ by using differential adsorption calorimetry will be required to resolve the problem. Experimental work in this area has started to emerge. The published data are, however, still limited to pure and binary gas adsorption systems (Dunne et al., 1997).

### *Adsorption kinetics*

Unlike adsorption equilibria, compilation and systematic analysis of pure and multicomponent gas adsorption kinetic data are absent from the published literature. In fact, the open literature contains only a few binary adsorption kinetic data (Karger and Ruthven, 1992; Ruthven, 1984). Kinetic studies of adsorption systems containing three or more components are rare. The following three reasons may explain the historic state of this subject:

(a) The diffusivities ($D_i$) or the mass-transfer coefficients ($k_i$) for adsorption of a pure gas $i$ or the component $i$ of a multicomponent gas mixture ($i = 1, 2, \ldots$) can be functions of the transient surface excesses of all components present in the system and the adsorbent temperature at a given location and time within the adsorbent mass during the kinetic ad(de)sorption process. Consequently, the database required to completely describe the kinetic process ($D_i$ or $k_i$ as functions of $n_i^m$ and $T$) can be extremely large.

(b) Several different simultaneous mass-transfer resistances (external gas film resistance, adsorbent surface barrier resistance, gas and surface phase diffusional resistances in mesopores of the adsorbent, and activated diffusional resistance in micropores) may control the overall adsorption kinetics (Ruthven, 1984). The structural (network of meso-micropores) and chemical (surface polarity, ionic nature of surface, and so on) heterogeneity of most practical adsorbents further complicates the mass-transfer process. These microscopic heterogeneities cannot generally be quantified using existing techniques, which complicates the analysis of the overall ad(de)sorption kinetics at a fundamental level.

Mathematical models can be developed to account for different mass-transfer mechanisms using a simplified structural description of the adsorbent. Models must also account for the local surface excess and temperature dependence of adsorbate diffusivities in order to explain the experimentally measured overall adsorption kinetics. These models usually have too many parameters to be evaluated unambiguously from the experimental kinetic data. The data interpretation, thus, often becomes very complicated and model-dependent. This complexity may have discouraged research in this area. A common practice is to describe the measured kinetic data in terms of an overall transport parameter.

(c) The commonly used methods for measurement of ad(de)sorption kinetics such as gravimetric adsorption technique (GAT) for pure gas and volumetric adsorption technique (VAT) for pure and multicomponent gas mixtures are generally nonisothermal processes. The GAT uses a microbalance which monitors the transient weight change of the adsorbent mass during the adsorbate uptake (loss) process (Ross and Olivier, 1964). The VAT experiment for kinetics is identical to that for equilibrium measurement except that the gas-phase pressure and compositions are measured as functions of time. In both cases, transient mass balances allow the calculation of $n_i^m$ as functions of time ($t$).

Heat is evolved (consumed) during the ad(de)sorption process, which cannot generally be removed (supplied) instantaneously from the system, causing the temperature of the adsorbent to rise (fall). Consequently, coupled mass and heat balance equations for the system must be solved in order to estimate $D_i$ or $k_i$ from the experimental data. This can enormously complicate data analysis for multicomponent ($i > 2$) adsorption systems. The problem is severe when an integral step change in the gas-phase pressure or composition is applied during the kinetic test, because it causes a large change in adsorbate surface excesses and adsorbent temperatures and the dependence of mass-transfer coefficients on those variables are generally unknown. A differential step change in gas-phase pressure or composition during the kinetic test (small change in adsorbent temperature and adsorbate surface excess) significantly simplifies the mathematical mass-heat-transfer modeling and their solutions (Ruthven, 1984; Sircar, 1983, 1994) by permitting (1) the use of constant values of $D_i$ or $k_i$ at the base values of $T$ and $n_i^m$ of the test and (2) linearization of the adsorption equilibria with respect to $P$, $T$ and $y_i$. *A-priori* estimation of the governing heat-transfer mechanism (and heat-transfer coefficient) for the nonisothermal kinetic tests may not be easy and can intro-

duce ambiguity about the estimated mass-transfer coefficients. These nonisothermal effects of the conventional adsorption kinetic tests are often not recognized and system isothermality is erroneously assumed, particularly for the differential tests.

### *Adsorbent regeneration*

Adsorption equilibrium, isosteric heats, and kinetics of pure and multicomponent gas systems can be substantially altered by the presence of trace quantities of strongly co-adsorbed components such as water on polar adsorbents (Breck, 1984). The quantity of preadsorbed trace component is determined by the adsorbent regeneration temperature, rate and duration of inert regeneration gas flow over the adsorbent. It is necessary that the adsorbent regeneration conditions be rigorously reproduced before data from different sources are compared. Identical adsorbent regeneration is also required for comparing bench scale and industrial scale adsorptive process performances.

## Data Reproducibility

Adsorption equilibrium and kinetic data for the same gas-solid systems from different laboratories around the world often do not match with one another. Inconsistent adsorbent regeneration procedures, subtle differences in the adsorbent structure, thermal intrusion during kinetic experiments and the differences in the mode of data analysis (model interpretation) are often the primary causes of the mismatch. In general, more agreement is found for the thermodynamic equilibrium data than the kinetic data from different sources. An order of magnitude difference in the estimated values of adsorbate transport properties is often considered to be acceptable. This degree of uncertainty is, however, not tolerable for practical process designs.

## Isotope Exchange Technique

The isotope exchange technique (IET) for measurement of pure and multicomponent gas adsorption equilibria and kinetics can resolve some of the problems encountered by conventional measurement methods described earlier. The general principle of IET consists of equilibrating (saturating) an adsorbent mass with a pure adsorbate at a given $P$ and $T$ or with a multicomponent gas mixture ($i \geq 2$) at a given $P$, $T$, and $y_i$. The corresponding equilibrium surface excess of component $i$ is $n_i^m$. The pure gas $i$ or the component $i$ of the multicomponent system may consist of a mixture of a bulk isotope (mole fraction $y_i^{*0}$) and one or more dilute or trace isotopes ($j$ varieties) having mole fractions of $y_{ij}^{*0}$:

$$y_i^{*0} + \sum_j y_{ij}^{*0} = 1 \qquad \text{Pure Gas} \tag{1}$$

$$y_i^{*0} + \sum_j y_{ij}^{*0} = y_i \qquad i, j = 1, 2, \ldots, \text{Multicomponent gas} \tag{2}$$

The equilibrated adsorbate-adsorbent system is then contacted with another pure gas or gas mixture at identical conditions of $P$, $T$, and $y_i$ except that the component $i$ isotope mole fractions ($y_i^{*s}$ and $y_{ij}^{*s}$) of the second gas are different from those of the first. A chemical potential driving force for transport is created for the different isotopic species of component $i$ (gas to adsorbed phase (adsorption) and adsorbed to gas phase (desorption) depending on whether $y_i^{*s} \gtrless y_i^{*0}$ or $y_{ij}^{*s} \gtrless y_{ij}^{*0}$) until a new isotopic equilibrium state is created having a gas-phase mole fraction of $y_i^{*\infty}$ and $y_{ij}^{*\infty}$. The total mole fraction of component $i$ remains constant at $y_i$ during the entire exchange process. Thus,

$$y_i^*(t) + \sum_j y_{ij}^*(t) = y_i^{*s} + \sum_j y_{ij}^{*s} = y_i^{*\infty} + \sum_j y_{ij}^{*\infty} = 1 \quad \text{Pure gas} \tag{3}$$

$$y_i^*(t) + \sum_j y_{ij}^*(t) = y_i^{*s} + \sum_j y_{ij}^{*s} = y_i^{*\infty} + \sum_j y_{ij}^{*\infty} = y_i$$

$$i = 1, 2, \ldots, \text{Multicomponent gas} \tag{4}$$

where $y_i^*(t)$ and $y_{ij}^*(t)$ are the gas-phase mole fractions of the bulk and the dilute $j$th isotopes of component $i$ at time $t$ during the exchange process. The kinetics of the exchange process can be measured by monitoring $y_i^*(t)$ and $y_{ij}^*(t)$.

There is no driving force for transport of component $i$ as a whole (constant $P$, $T$ and $y_i$). Thus, the adsorption equilibria for component $i$ ($n_i^m$) of the pure gas or the gas mixture remains undisturbed during the process. The transport of the isotopic species of component $i$ are governed by the self-diffusion mechanisms under constant $P$, $T$ and $y_i$ or $n_i^m$ and $T$. These mechanisms, however, can be different for different adsorbate-adsorbent systems.

It will be demonstrated later that the above described IET can be used to *simultaneously* measure the pure or multicomponent adsorption equilibria ($n_i^m$ as functions of $P$, $T$ and $y_i$) and kinetics (transport coefficients for self-diffusion of component $i$ as functions of $n_i^m$ and $T$) of each component $i$ in the system in a single experiment. The other key advantages of the method are as follows:

(a) Complete control over the equilibrium state of the adsorption system (determined by the choice of the variables $P$, $T$ and $y_i$ in the experiment).

(b) Absolutely isothermal process (equilibrium state is not disturbed during the process).

(c) Experimental replicability (experiment can be repeated many times by varying $y_i^{*s}$ and $y_{ij}^{*s}$ while maintaining the same equilibrium state).

(d) Relative ease of experimental procedure (compared to TDT).

The IET concept has been extensively used in the past by various research groups for exclusively measuring the self-diffusion of pure adsorbates in porous adsorbents. A variety of gas contact systems such as VAT, GAT, column dynamic method, zero length chromatography, and closed-loop recycling method have been used. Table 1 lists some of the key experimental works.

Another class of experimental methods using the IET concept is called the tracer-pulse chromatography (TPC). The adsorption equilibria for the adsorbates ($n_i^m$ as functions of $P$, $T$ and $y_i$) can be estimated by analyzing the first moment of the chromatographic response for the isotope, and the adsorbate transport properties for self-diffusion can be analyzed from the second moment of the response. The analysis

**Table 1. Key Published Works on Isotope Exchange Methods for Study of Adsorption**

| Authors | Experimental Method | System Studied | Comments |
|---|---|---|---|
| Morikawa and Ozaki (1968) | Closed-loop recycling | Displacement of adsorbed $N_2$ isotope from iron promoted catalyst by ordinary $N_2$ | Time course of displacement measured by exchange of pure $N_2^{28}$ and $N_2^{30}$ |
| Quig and Rees (1976) | Closed-loop recycling | Kinetics of self-diffusion of pure $C_5$–$C_9$ alkanes on Ca-Na-A zeolite | Exchange between pure deuterated and undeuterated hydrocarbons |
| Takeuchi and Kawazoe (1976) | Column dynamics | Breakthrough curves for displacing ordinary $CO_2$ by isotopic $CO_2$ on 4-Å, 5-Å, and 13X zeolites | Nitrogen used as carrier gas for $CO_2$; exchange between $C^{12}O_2$ and $C^{14}O_2$ |
| Nanba, Oishi and Ando (1982) | Volumetric adsorption | Pure $O_2^{32}$ displaced by pure $O_2^{36}$ | Theoretical model including transfer resistance in the solid (plane sheet) and external film diffusion |
| Goddard and Ruthven (1986) | Gravimetric adsorption | Self-diffusion of pure $C_8$ aromatic hydrocarbon on Faujasite-type zeolite | Exchange between pure hydrogen and deuterated forms of $C_8$ hydrocarbon |
| Forste, Karger and Pfeiffer (1989) | NMR tracer uptake | Self-diffusion of pure benzene in ZSM-5 and NaX zeolites | Exchange between pure hydrogen and deuterated form of benzene |
| Dutel, Seibold and Gelin (1991) | Transient isotopic chromatography | Self-diffusion of pure methanol and methane in MFI zeolite | Exchange between pure hydrogen and deuterated forms of hydrocarbons |
| Brandani, Hufton and Ruthven (1995) | Zero length chromatography | Self-diffusion of pure propane and propylene in 5-Å and 13X zeolites | Helium used as carrier gas; exchange between hydrogen and deuterated forms of hydrocarbons |
| Helfferich and Peterson (1963) | Tracer-pulse chromatography | No experiment | Concept of measurement of multicomponent equilibria by TPC |
| Peterson, Helfferich and Carr (1966) | Tracer-pulse chromatography | Pure gas equilibrium of $CH_4$ on activated carbon and $C_7H_{16}$ on 5-Å zeolite | No carrier gas. Radio-tracer of hydrocarbons used |
| Hyun and Danner (1985) | Tracer-pulse chromatography | Pure gas equilibrium and self-diffusion of ethane and ethylene on 13X zeolite | Radio isotopes of ethane and ethylene used as tracer pulse gas |
| Hufton and Danner (1991) | Tracer-pulse chromatography | Equilibrium and kinetics of pure ethane on silicalite | Uses a carrier gas and radioactive tracer of hydrocarbon |

of the second moment, however, can be very complicated and ambiguous due to axial dispersion, column pressure drop (for small adsorbent particles), and, in general, its dependency on the chosen mass-transfer model. Published TPC studies are also limited to single adsorbate systems. Table 1 lists some of the key works in this area.

The self-diffusion of adsorbates measured by all of the above IET methods correspond to the transport of adsorbate molecules from the gas phase to the adsorbed phase within the adsorbent mass and vice versa. Self-diffusion of adsorbate molecules within the adsorbent mass itself can be measured by the pulsed field gradient NMR technique (Karger and Ruthven, 1992).

## Experimental Method

We now describe the IET used in our laboratory. The experimental apparatus and the data collection method are similar to those used by Quig and Rees (1976). It consists of a closed-loop gas recirculating adsorption apparatus described by Figure 1. The main loop consists of an adsorbent chamber (with valves $V_1$ and $V_2$), a gas circulating bellows pumps, two multiport valves (A and B), and pressure transducers (P1 and P2) which measure gas-phase pressures at the inlet and outlet of the adsorption chamber. A third pressure transducer (P3) measures the pressure of the dosing loop. The temperature of the adsorbent in the chamber can be measured by a thermocouple (TC). A quadrapole mass spectrometer continuously withdraws a very small quantity of gas (0.33 std. $cm^3/h$) from the main loop for analysis of isotope concentrations in the gas phase. A loop of known volume is attached to the multiport valve B for introducing the dosing gas into the main loop. The entire apparatus is thermostated in an air bath (constant temperature $T$) with a temperature control of $\pm 0.1°C$.

A quantity (1–10 g) of the regenerated adsorbent was packed into the adsorbent chamber under an inert ($N_2$) at-

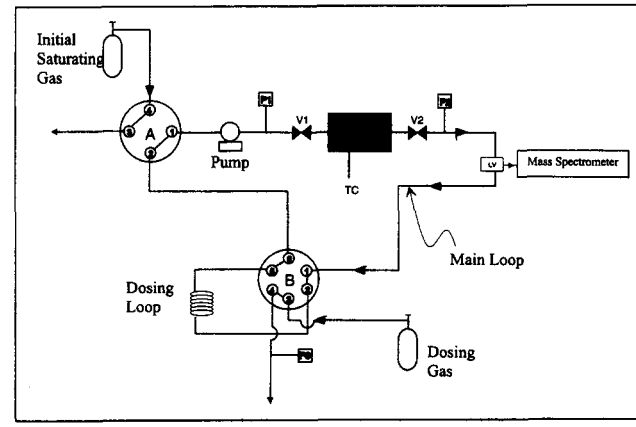


**Figure 1. Experimental apparatus for isotope exchange technique.**

mosphere inside a glove box and then the chamber was connected to the main loop with valves $V_1$ and $V_2$ closed. The $N_2$ was purged out of the chamber (open valves $V_1$ and $V_2$) by flowing inert helium through multiport valves A and B and the main loop. The specific helium void volume ($V_m = 10.0$ cc/g of adsorbent) of the main loop with the adsorbent in place was measured by expanding helium at a higher pressure from the dosing loop into the main loop and measuring the pressure changes. The main loop was then evacuated and the pure and multicomponent saturating gas at $P$, $T$, and $y_i$ was introduced into the main loop through valve A. The flow of this gas through the system was continued until the adsorbent was saturated with the inlet gas. The isotopic mole fractions of component $i$ of the saturating gas were, respectively, $y_i^{*0}$ and $y_{ij}^{*0}$, for the bulk and the trace $j$th isotope of component $i$ as measured by the mass spectrometer. The pump was started and the gas in the main loop was circulated at a rate of $\sim 500$ cc/min. Control experiments showed that the kinetic measurements were independent of flow rate above 400 cc/min. The dosage loop was then filled with another pure gas or mixture at $P$, $T$ and $y_i$ through valve B. The isotope mole fractions of component $i$ in the dosage loop gas were, respectively, $y_i^{*d}$ and $y_{ij}^{*d}$, for the bulk and trace $j$th isotope of component $i$. Finally, the dosage loop (specific volume $V_d = 0.0625$ cm$^3$/g of adsorbent) was connected with the main loop (time $t = 0$) through valve B and the entire gas (specific volume $V = V_d + V_m$, cm$^3$/g of adsorbent) in the system was circulated over the adsorbent. The changes in the gas-phase mole fractions of the isotopes of component $i$ [bulk isotope, $y_i^*(t)$; dilute $j$th isotope $y_{ij}^*(t)$] were monitored as functions of $t$ using the mass spectrometer until they reached constant values of $y_i^{*\infty}$ and $y_{ij}^{*\infty}$. About 15 s was required to mix the dosed and main loop gases.

## Data Analysis

### *Adsorption equilibria*

We us the Gibbsian surface excesses, which are the only true experimental variables, to define the extents of adsorption of the different isotope species of component $i$ as well as those for the total component $i$ (Sircar, 1985, 1996). Thus, at any time $t$ during the above described isotope exchange process

$$n_i^m = n_i - \nu^a \rho y_i \qquad i = 1,2,\ldots \tag{5}$$

$$n_i^{*m}(t) = n_i^*(t) - \nu^a \rho y_i^*(t) \qquad i = 1,2,\ldots \tag{6}$$

$$n_{ij}^{*m}(t) = n_{ij}^*(t) - \nu^a \rho y_{ij}^*(t) \qquad i,j = 1,2,\ldots \tag{7}$$

where $n_i^m$, $n_i^{*m}(t)$ and $n_{ij}^{*m}(t)$ are, respectively, the specific Gibbsian surface excesses (mol/g of adsorbent) of total component $i$, the bulk isotope component of $i$ and the dilute $j$th isotope of component $i$ at any time $t$. The variables $n_i$ [$= (n_i^* + \Sigma_j n_{ij}^*)$], $n_i^*$ and $n_{ij}^*$ are the corresponding specific actual amounts adsorbed (mol/g of adsorbent) at any time $t$. The specific adsorbed phase volume (cm$^3$/g of adsorbent) and the gas-phase density (mol/cm$^3$) at time $t$ are given by $\nu^a$ and $\rho$, respectively. The variables $\nu^a$, $\rho$, $n_i^m$ and $n_i$ remain constant during the experiment because $P$, $T$ and $y_i$ are constants. It follows from Eqs. 3, 4, and 5–7 that

$$n_i^m = n_i^{*m}(t) + \sum_j n_{ij}^{*m}(t) \tag{8}$$

The total specific amounts (mol/g of adsorbent) of the component $i$ ($\bar{n}_i$), the bulk isotope of component $i$ ($\bar{n}_i^*$), and the dilute isotope of species $j$ of component $i$ ($\bar{n}_{ij}^*$) in the entire system after the dosing and main loops are connected ($t \geq 0$) are given by

$$\bar{n}_i = n_i^m + V\rho y_i \qquad i = 1,2,\ldots \tag{9}$$

$$\bar{n}_i^* = n_i^{*m}(t) + V\rho y_i^*(t) \qquad i = 1,2,\ldots \tag{10}$$

$$\bar{n}_{ij}^* = n_{ij}^{*m}(t) + V\rho y_{ij}^*(t) \qquad i = 1,2,\ldots \tag{11}$$

Quantities $\bar{n}_i$, $\bar{n}_i^*$ and $\bar{n}_{ij}^*$ remain constant during the experiment provided that the adsorbent does not initiate a reaction between the isotopes of component $i$ creating new isotopic species.

A simple mass balance for each isotope of component $i$ in the entire system yields ($t \geq 0$)

$$\bar{n}_i^* = n_i^{*m}(0) + V\rho y_i^{**} = n_i^{*m}(\infty) + V\rho y_i^{*\infty} \qquad i = 1,2,\ldots \tag{12}$$

$$\bar{n}_{ij}^* = n_{ij}^{*m}(0) + V\rho y_{ij}^{**} = n_{ij}^{*m}(\infty) + V\rho y_{ij}^{*\infty} \qquad i,j = 1,2,\ldots \tag{13}$$

$$\bar{n}_i = \bar{n}_i^* + \sum_j \bar{n}_{ij}^* \qquad i,j = 1,2,\ldots \tag{14}$$

where $n_i^{*m}(0)$ and $n_{ij}^{*m}(0)$ are, respectively, the surface excesses of the bulk and the dilute $j$th isotopes of component $i$ at $t \leq 0$ (equilibrium surface excesses at $P$, $T$, $y_i^{*0}$ and $y_{ij}^{*0}$). $y_i^{**}$ and $y_{ij}^{**}$ are the gas-phase mole fractions of the bulk and the dilute $j$th isotopes of component $i$ at $t = 0$. They are given by

$$y_i^{**} = \left[\frac{V_m y_i^{*0} + V_d y_i^{*d}}{V}\right] \qquad i = 1,2,\ldots \tag{15}$$

$$y_{ij}^{**} = \left[\frac{V_m y_{ij}^{*0} + V_d y_{ij}^{*d}}{V}\right] \qquad i,j = 1,2,\ldots \tag{16}$$

The variables $n_i^{*m}(\infty)$ and $n_{ij}^{*m}(\infty)$ are, respectively, the equilibrium surface excesses of the bulk isotope and the dilute $j$th isotope of component $i$ at $P$, $T$, $y_i^{*\infty}$ and $y_{ij}^{*\infty}$.

We assume (a) that the pure gas equilibrium adsorption isotherms of all isotope species of component $i$ are identical and (b) that the experimental equilibrium selectivities [$S_{i-ij}^{*m} = n_i^{*m} y_{ij}^* / n_{ij}^{*m} y_i^*$] of adsorption (Sircar, 1996) between the bulk isotope of component $i$ and the dilute $j$th isotope species of component $i$ are unity in the absence or presence of other components of the gas mixture. Thus, one may write

$$\frac{n_i^{*m}(0)}{y_i^{*0}} \cdot \frac{y_{ij}^{*0}}{n_{ij}^{*m}(0)} = 1 \qquad i,j = 1,2,\ldots \tag{17}$$

$$\frac{n_i^{*m}(\infty)}{y_i^{*\infty}} \cdot \frac{y_{ij}^{*\infty}}{n_{ij}^{*m}(\infty)} = 1 \qquad i,j = 1,2,\ldots \tag{18}$$

It follows from Eqs. 17 and 18 that

$$\frac{n_i^{*m}(0)}{y_i^{*0}} = \frac{n_{ij}^{*m}(0)}{y_{ij}^{*0}} = C_0 \qquad i,j = 1,2,\ldots \tag{19}$$

$$\frac{n_i^{*m}(\infty)}{y_i^{*\infty}} = \frac{n_{ij}^{*m}(\infty)}{y_{ij}^{*\infty}} = C_\infty \qquad i,j = 1,2,\ldots \tag{20}$$

where $C_0$ and $C_\infty$ are constants.

Equations 1–4, 8, 19 and 20 can be combined to get

$$\frac{n_i^m}{y_i} = \frac{n_i^{*m}(0)}{y_i^{*0}} = \frac{n_{ij}^{*m}(0)}{y_{ij}^{*0}} = C_0 \qquad i,j = 1,2,\ldots \tag{21}$$

$$\frac{n_i^m}{y_i} = \frac{n_i^{*m}(\infty)}{y_i^{*\infty}} = \frac{n_{ij}^{*m}(\infty)}{y_{ij}^{*\infty}} = C_\infty \qquad i,j = 1,2,\ldots \tag{22}$$

Thus, $C_0$ and $C_\infty$ are equal ( $= C$).

It can be easily shown from Eqs. 5–7 that under the condition of operation of IET (undisturbed adsorbed phase), the equilibrium selectivities based on actual amounts adsorbed [$S_{i-ij}^* = n_i^* y_{ij}^* / n_{ij}^* y_i^*$] between the bulk and the $j$th isotopes of component $i$ are also equal to unity when the measured selectivities ($S^{*m}$) are assumed to be unity. The quantities $S_{i-ij}^*$ are, however, not experimental variables (Sircar, 1996).

Equations 12, 13, 21, and 22 can be combined to get

$$n_i^m(P, T, y_i) = (V\rho) y_i \left[\frac{y_i^{**} - y_i^{*\infty}}{y_i^{*\infty} - y_i^{*0}}\right] = (V\rho) y_i \left[\frac{y_{ij}^{**} - y_{ij}^{*\infty}}{y_{ij}^{*\infty} - y_{ij}^{*0}}\right] \qquad i,j = 1,2,\ldots \tag{23}$$

Equations 15, 16 and 23 show that the equilibrium surface excess of component $i$ ($n_i^m$) at a given $P$, $T$, $y_i$ can be calculated by measuring $V_m$, $V_d$, $\rho(P, T)$, $y_i$, $y_i^{*0}$ or $y_{ij}^{*0}$, $y_i^{*d}$ or $y_{ij}^{*d}$, and $y_i^{*\infty}$ or $y_{ij}^{*\infty}$ by the above described IET. The measurement of the initial (main and dose loop) and final gas-phase isotopic mole fractions of either the bulk isotope of component $i$ ($y_i^*$) or any one or more of the dilute $j$th isotope of component $i$ ($y_{ij}^*$) is sufficient. It may be desirable to use the gas-phase mole fractions of one of the trace isotope species of component $i$, which can be monitored most reliably by the mass spectrometer in Eq. 23.

This IET allows simultaneous measurement of equilibrium surface excesses ($n_i^m$, $i = 1, 2, \ldots$) of all components of a multicomponent gas mixture ($i \geq 2$) at a given $P$, $T$, and $y_i$ by simultaneously monitoring the mole fractions of the isotopic species of different components ($i = 1, 2, \ldots$) of the gas mixture in a single experiment. This method significantly simplifies the experimental protocol and reduces the time requirement for measurement of multicomponent gas adsorption equilibria. There is also the added advantage of infinite data replicability without much difficulty. These powerful advantages of measuring multicomponent gas adsorption equilibria by IET were not recognized before.

### *Adsorption kinetics*

The total flux ($J_i$) of component $i$ (pure gas or mixture) in the IET is equal to zero because there is no overall chemical potential driving force for component $i$ (constant $P$, $T$, $y_i$). The fluxes of the bulk isotope of component $i$ ($J_i^*$) and the dilute $j$th isotope of component $i$ ($J_{ij}^*$) are, however, finite. Thus

$$J_i = J_i^* + \sum_j J_{ij}^* = 0 \qquad i,j = 1,2,\ldots \tag{24}$$

Thus, some of the isotopes of component $i$ are adsorbing while the others are desorbing. One can define fractional uptakes (losses) of the isotopes of component $i$ as functions of time by

$$f_i^*(t) = \frac{n_i^{*m}(t) - n_i^{*m}(0)}{n_i^{*m}(\infty) - n_i^{*m}(0)} = \frac{y_i^{**} - y_i^*(t)}{y_i^{**} - y_i^{*\infty}} \qquad i = 1,2,\ldots \tag{25}$$

$$f_{ij}^*(t) = \frac{n_{ij}^{*m}(t) - n_{ij}^{*m}(0)}{n_{ij}^{*m}(\infty) - n_{ij}^{*m}(0)} = \frac{y_{ij}^{**} - y_{ij}^*(t)}{y_{ij}^{**} - y_{ij}^{*\infty}} \qquad i,j = 1,2,\ldots \tag{26}$$

where $f_i^*(t)$ and $f_{ij}^*(t)$ are fractional uptake (losses) of the bulk isotope of component $i$ and dilute $j$th isotope of component $i$, respectively, at time $t$. The righthand side terms of Eqs. 25 and 26 follow from Eqs. 10 and 14. They show that $f_i^*(t)$ and $f_{ij}^*(t)$ can be measured as functions of time by measuring gas-phase mole fractions of the isotopes of component $i$. Simultaneous estimation of fractional uptakes or losses of one or more isotopes of each component of the system can be carried out in a single experiment at constant $P$, $T$, and $y_i$ (or constant $n_i^m$, $T$). The rate of change of transient surface excesses of the isotopes of component $i$ can be easily obtained from Eqs. 10, 11, 25, and 26 as

$$\frac{dn_i^{*m}(t)}{dt} = -(V\rho)\frac{dy_i^*(t)}{dt} \qquad i = 1,2,\ldots \tag{27}$$

$$\frac{dn_{ij}^{*m}(t)}{dt} = -(V\rho)\frac{dy_{ij}^*(t)}{dt} \qquad i,j = 1,2,\ldots \tag{28}$$

The variables on the righthand side of Eqs. 27 and 28 can be experimentally measured.

The equilibrium line for the isotope of component $i$ during the exchange process can also be easily estimated. We assume that $n_i^{*m}(e)$ and $n_{ij}^{*m}(e)$ are, respectively, the equilibrium surface excesses of the bulk isotope of component $i$ and the dilute $j$th isotope of component $i$ corresponding to the gas-phase mole fractions of these isotopes at any time $t$. Invoking the assumption of unity selectivity between the bulk and dilute isotopes of component $i$, one has

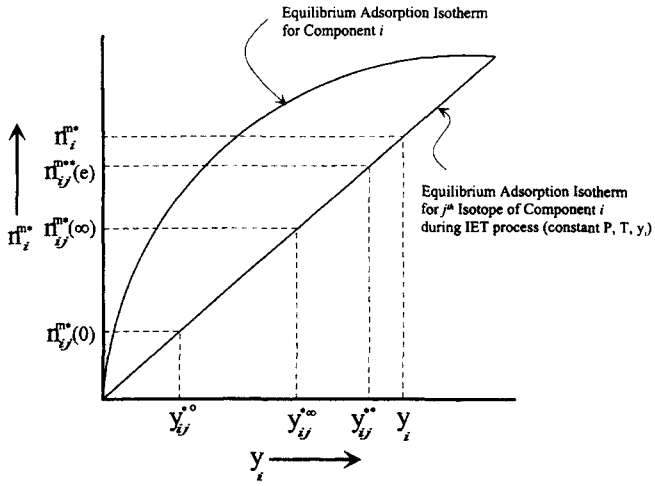


**Figure 2. Equilibrium line for isotope exchange process.**

$$\frac{n_i^{*m}(e)}{n_{ij}^{*m}(e)} \cdot \frac{y_{ij}^*(t)}{y_i^*(t)} = 1 \qquad i,j = 1,2,\ldots \tag{29}$$

It follows from Eq. 29 that

$$\frac{n_i^{*m}(e)}{y_i^*(t)} = \frac{n_{ij}^{*m}(e)}{y_{ij}^*(t)} = C_e \qquad i,j = 1,2,\ldots \tag{30}$$

where $C_e$ is a constant. Again, it follows from Eqs. 1–4, 21, 22, and 30 as well as the constancy of $n_i^m$ $[= n_i^{*m}(e) + \Sigma_j n_{ij}^{*m}(e)]$ that $C_e = C$. In other words,

$$n_i^{*m}(e) = y_i^*(t) \cdot \frac{n_i^m}{y_i} \tag{31}$$

$$n_{ij}^{*m}(e) = y_{ij}^*(t) \cdot \frac{n_i^m}{y_i} \tag{32}$$

Equations 31 and 32 show a very important property of the IET. Figure 2 depicts the equilibrium line for the $j$th isotope of component $i$ during the exchange process. The equilibrium surface excesses of the isotopes of component $i$ (corresponding to the gas-phase isotope mole fractions of component $i$ at any time $t$ during the exchange process) are proportional to the gas-phase isotope concentrations of component $i$ at that time.

## Specific Mass-Transfer Models

The following sections provide the analytical solutions for the experimental uptake (loss) curves for the $j$th isotope of component $i$ using different mass-transfer models:

### *Linear driving force (LDF) model*

The rate of change of surface excess of dilute $j$th isotope of component $i$ at time $t$ is given by

$$\frac{dn_{ij}^{*m}(t)}{dt} = k_{ij}^*[n_{ij}^{*m}(e) - n_{ij}^{*m}(t)] \qquad i,j = 1,2,\ldots \tag{33}$$

where $n_{ij}^{*m}(t)$ is the transient surface excess of the dilute $j$th isotope species of component $i$ at time $t$ and $n_{ij}^{*m}(e)$ is the corresponding surface excess in equilibrium with the gas-phase mole fraction of $y_{ij}^*$ at time $t$. $k_{ij}^*$ ($s^{-1}$) is the mass-transfer coefficients for self-diffusion of dilute $j$th isotope species. Equations 11, 13, 22, 23, 26, 28, 32, and 33 can be combined and integrated to get

$$\ln[1 - f_{ij}^*(t)] = -(k_{ij}^* a_{ij}^*)t \qquad i,j = 1,2,\ldots \tag{34}$$

$$a_{ij}^* = \left[\frac{y_{ij}^{**} - y_{ij}^{*0}}{y_{ij}^{*\infty} - y_{ij}^{*0}}\right] \qquad i,j = 1,2,\ldots \tag{35}$$

Equations 34 and 35 describe the variation in fractional uptake (loss) of the dilute $j$th isotope of component $i$ with time by the LDF model.

A certain amount of time ($t^*$, ~15s) may be needed by the above-described IET in order to mix the dosing gas with the main loop gas after contact ($t = 0$). The mole fractions of the isotopes of component $i$ may fluctuate during this period. The isotope mole fractions reach values of $y_i^*(t^*)$ and $y_{ij}^*(t^*)$ at the end of this period and then they smoothly change to $y_i^{*\infty}$ and $y_{ij}^{*\infty}$. Equation 34 can be rewritten to describe $f_{ij}^*$ as function of time ($t \geq t^*$) as

$$\ln\left[\frac{1 - f_{ij}^*(t)}{1 - f_{ij}^*(t^*)}\right] = -(k_{ij}^* a_{ij}^*)(t - t^*) \qquad i,j = 1,2,\ldots \tag{36}$$

A plot of the quantity of the lefthand side of Eq. 36 against $(t - t^*)$ should be linear with a negative slope of $(k_{ij}^* a_{ij}^*)$. Thus, $k_{ij}^*$ can be extracted from the experimental data.

### *Phase exchange reaction (PER) model*

The isotope exchange process can be described as an equimolar reaction between the isotopes of component $i$ in the gas ($g$) and adsorbed ($a$) phases. Thus

$$ij^*(g) + i^{*R}(a) \Leftrightarrow ij^*(a) + i^{*R}(g) \qquad i,j = 1,2,\ldots \tag{37}$$

Equation 37 states that one mol of the dilute $j$th isotope of component $i$ in the gas phase $[ij^*(g)]$ reacts with one mol of all other adsorbed isotope species of component $i[i^{*R}(a)]$ to form one mol of adsorbed $j$th isotope species of component $i$ $[ij^*(a)]$ and one mol of all other isotopes of component $i$ in the gas phase $[i^{*R}(g)]$. By using the laws of mass action, one can describe the rate process of Eq. 37 by

$$\frac{dn_{ij}^{*m}(t)}{dt} = k_{ij}^{*f}[n_i^m - n_{ij}^{*m}(t)][Py_{ij}^*(t)] - k_{ij}^{*b}[n_{ij}^{*m}(t)][P\{y_i - y_{ij}^*(t)\}] \tag{38}$$

where $k_{ij}^{*f}$ and $k_{ij}^{*b}$ ($s^{-1} \cdot atm^{-1}$) are, respectively, the forward and backward reaction rate constants for Eq. 37. The

surface excess variables are used to describe the extents of adsorption of different components in Eq. 38.

If the system were at equilibrium at time $t[n_{ij}^{*m}(t) = n_{ij}^{*m}(e)]$, the rate of change of $n_{ij}^{*m}$ would be equal to zero, and

$$k_{ij}^{*f} = k_{ij}^{*b} = \bar{k}_{ij}^{*} \tag{39}$$

It also follows from Eqs. 32, 38 and 39 that

$$\frac{[n_i^m - n_{ij}^{*m}(e)]}{n_i^m} = \left[\frac{y_i - y_{ij}^{*}}{y_i}\right] \tag{40}$$

$$\frac{dn_{ij}^{*m}}{dt} = \bar{k}_{ij}^{*}[Py_i][n_{ij}^{*m}(e) - n_{ij}^{*m}(t)] \tag{41}$$

Equation 39 shows that the forward and backward reaction rate constants for isotope $j$ of component $i$ are equal. It also follows from Eqs. 33 and 41 that the LDF and the PER models are equivalent for the IET process with $[k_{ij}^{*} = \bar{k}_{ij}^{*}(Py_i)]$. Thus, the analytical solution for uptake (Eqs. 34–36) also applies for the PER model.

### *Chemical potential driving force (CDPF) model*

Consider the transient isothermal diffusion of the $j$th isotope of component $i$ into a spherical porous (homogeneous) adsorbent particle of radius $a$ which is initially equilibrated with a multicomponent gas mixture at $P$, $T$, and $y_i$. The flux $J_{ij}^{*}(r,t)$ of the $j$th isotope of component $i$ (mol/cm$^2$/s) at time $t$ and radius $r$ of the adsorbent particle is given by the CPDF model as (Barrer, 1971)

$$J_{ij}^{*}(r,t) = -B_{ij}^{*}C_{ij}^{*}(r,t)\left[\frac{\delta\{\mu_{ij}^{*}(r,t)/RT\}}{\delta r}\right]_t \qquad 0 \le r \le a \tag{42}$$

where $B_{ij}^{*}$ (cm$^2$/s) is the mobility of the $j$th isotope of component $i$ at $P$, $T$ and $y_i$ (or $n_i^m$ and $T$). $C_{ij}^{*}(r,t)$ and $\{\mu_{ij}^{*}(r,t)/RT\}$ are, respectively, the total molar concentration (mol/cm$^3$) and the dimensionless chemical potential of the $j$th isotope of component $i$ at $r$ and $t$ within the particle. $R$ is the gas constant, and $\mu_{ij}^{*}(r,t)/RT$ is the true driving force for transport of the $j$th isotope according to irreversible thermodynamics (Callen, 1965) and it increases with increasing $r$ for the present diffusional process. Equation 42 assumes that there is no contribution in the flux of the $j$th isotope of component $i$ due to chemical potential gradients of the isotopic species of other components (absence of cross terms for flux). The variable $C_{ij}^{*}(r,t)$ can be expressed as

$$C_{ij}^{*}(r,t) = \rho_p[n_{ij}^{*m}(r,t) + \vartheta_p \rho y_{ij}^{*}(r,t)] \tag{43}$$

where $n_{ij}^{*m}(r,t)$ and $y_{ij}^{*}(r,t)$ are, respectively, the instantaneous specific surface excess (mol/g) and gas-phase mol fraction of the $j$th isotope of component $i$ at radius $r$ within the particle. $\vartheta_p$ (cm$^3$/g), $\rho_p$ (g/cm$^3$), and $\rho$ (mol/cm$^3$) are, respectively, the specific pore volume of the adsorbent, the adsorbent particle density, and the gas-phase density of the system.

Consider a gas phase at $P$, $T$ and $y_i$, which is in equilibrium with the adsorbent particle where the total adsorbate concentration of the $j$th isotope of component $i$ is $C_{ij}^{*}$. The equilibrium gas-phase mol fraction of the $j$th isotope of component $i$ is $y_{ij}^{*}(e)$. $y_{ij}^{*}(e)$ is a function of $r$ and $t$. Then, from equilibrium thermodynamics (Prausnitz, 1969)

$$\mu_{ij}^{*}(r,t) = \mu_{ij}^{*0}(T) + RT \ln Py_{ij}^{*}(e) \tag{44}$$

$\mu_{ij}^{*0}(T)$ is the pure component gas-phase chemical potential of isotope $j$ of component $i$ at temperature $T$ and pressure of one atmosphere. It also follows that

$$C_{ij}^{*}(r,t) = \rho_p[n_{ij}^{m*}(e) + \vartheta_p \rho y_{ij}^{*}(e)] \tag{45}$$

where $n_{ij}^{m*}(e)$ is the equilibrium specific surface excess (mol/g) of the $j$th isotope of component $i$ in equilibrium with a gas phase at $P$, $T$ and $y_i$ where the gas-phase mol fraction of the $j$th isotope of component $i$ is $y_{ij}^{*}(e)$.

Equation 32 (a constraint of IET) is used to determine $n_{ij}^{m*}(e)$. Equation 45 reduces to

$$C_{ij}^{*}(r,t) = K_i y_{ij}^{*}(e) \qquad i,j = 1,2,\ldots \tag{46}$$

where $K_i[= \rho_p\{(n_i^m/y_i) + \vartheta_p \rho\}]$ is a function of $P$, $T$ and $y_i$ (constant for a given IET experiment). Equations 42, 44 and 46 can be combined to get

$$J_{ij}^{*}(r,t) = -B_{ij}^{*}\left[\frac{\delta C_{ij}^{*}(r,t)}{\delta r}\right]_t \qquad i,j = 1,2,\ldots \tag{47}$$

Equation 47 shows that the flux of the $j$th isotope of component $i$ in the IET experiment can be described by the conventional Fickian Diffusion Model (FDM). The mobility variable ($B_{ij}^{*}$) is equivalent to the well-known Fickian Diffusivity ($D_{ij}^{*}$) for the $j$th isotope of component $i$. Reduction of Eqs. 42 to 47 is possible only because of the linear isotherm path (Eq. 32) of the exchange process. In general, $D_{ij}^{*}$ can be functions of $P$, $T$ and $y_{ij}^{*}$ (or $n_{ij}^{*m}$ and $T$).

An analytical solution of a mathematical model describing isothermal adsorbate uptake by the Fickian diffusion mechanism, where the adsorption process takes place from a well-stirred solution of limited volume (constant), is available (Crank, 1956). The model assumes that the adsorption system consists of a spherical adsorbent particle (radius = $a$) of volume $V_a$ (cm$^3$/g of adsorbent), which is immersed in a fluid phase of volume $V_b$ (cm$^3$/g of adsorbent). The entire adsorbent volume ($V_a$) is assumed to be the adsorbed phase. The adsorbent is initially equilibrated with a pure gas having a concentration of $c^{g_o}$ (mol/cm$^3$). The corresponding equi-

librium adsorbed phase concentration is $\bar{c}^o$ (mol/cm$^3$). The gas-phase adsorbate concentration is then changed to $c^{g*}$ at time zero. The adsorbate isothermally diffuses into the adsorbent particle following Fick's law (Eq. 47) until a new equilibrium state is formed. The final equilibrium gas and adsorbed phase adsorbate concentrations are given by $c^{g\infty}$ and $\bar{c}^\infty$, respectively. The time dependence of the fractional uptake of the adsorbate ($F$) is given by (Karger and Ruthven, 1992)

$$F(t) = \left[\frac{\bar{c}(t) - \bar{c}^o}{\bar{c}^\infty - \bar{c}^o}\right] = \left[\frac{c^{g*} - c^g(t)}{c^{g*} - c^{g\infty}}\right]$$

$$= 1 - \sum_{n=1}^{\infty} \frac{6\alpha(1+\alpha)e^{-\{Dq_n^2 t/a^2\}}}{9 + 9\alpha + q_n^2\alpha^2} \quad (48)$$

$$\tan q_n = \frac{3q_n}{3 + \alpha q_n^2} \quad (49)$$

$$\alpha = \left[\frac{c^{g\infty} - c^{go}}{c^{g*} - c^{g\infty}}\right] \quad (50)$$

where $c^g(t)$ and $\bar{c}(t)$ are, respectively, the gas and adsorbed phase adsorbate concentrations at time $t$. $D$ is the Fickian diffusivity of the adsorption. The parameter $[1/(1+\alpha)]$ represents the fraction of total moles of adsorbate introduced into the gas phase of the system $[V_b(c^{g*} - c^{go})]$ at time zero that is adsorbed $[V_a(\bar{c}^\infty - \bar{c}^o)]$ during the uptake process.

The above described model can be used to estimate the time constant $(D_{ij}^*/a^2)$ for self-diffusion of the $j$th isotope of component $i$ (at constant $P$, $T$, and $y_i$) into an adsorbent particle of radius $a$ using the fractional uptake data measured by IET. The adsorbent particle of the model, in this case, is initially equilibrated with a gas mixture at $P$, $T$ and $y_i$. The gas-phase mol fraction of the $j$th isotope of component $i$ is $y_{ij}^{*0}$. The gas-phase volume of the model system is $V(=V_b)$. The gas-phase mol fraction of the $j$th isotope of component $i$ is changed to a value of $y_{ij}^{**}$ at time equal to zero while maintaining the variables $P$, $T$ and $y_i$ constant. The $j$th isotope of component $i$ isothermally diffuses into the adsorbent particle following Fick's Law until a final equilibrium state characterized by $P$, $T$, $y_i$ and $y_{ij}^{*\infty}$ is formed. Equations 48–50 can then be used to estimate $[D_{ij}^*/a^2]$ by replacing the variables $c^{g*}$, $c^g(t)$, $c^{go}$, $c^{g\infty}$ and $D$ by $y_{ij}^{**}$, $y_{ij}^*(t)$, $y_{ij}^{*0}$, $y_{ij}^{*\infty}$ and $D_{ij}^*$, respectively.

Equations 48–50 are valid only for (a) the case of linear equilibrium adsorption isotherms for the adsorbate and (b) the constant value of $D$. Condition (a) is automatically satisfied by the IET. Condition (b) is satisfied when the difference between $y_{ij}^{**}$ and $y_{ij}^{*\infty}$ is small. These differences were typically 5,000 ppm for all of the experimental runs reported in this work.

Equations 4, 8, 43 and 47 show that one possible condition for satisfying Eq. 24 is

$$D_i^* = D_{ij}^* \qquad i, j = 1, 2, \ldots \quad (51)$$

where $D_i^*$ is the self-diffusion coefficient of the bulk isotope of component $i$ at $P$, $T$, and $y_i$. Thus, the self-diffusivities of the $j$th isotopes of component $i$ at $P$, $T$, and $y_i$ are equal to each other and they are also equal to the self-diffusivity of the bulk isotope of component $i$.

## Experimental Systems

We used the IET to measure equilibrium adsorption isotherms and self-diffusion coefficients of pure $N_2$ and $O_2$, as well as their binary mixtures on a commercial sample of pelletized carbon molecular sieve (CMS) and those for pure $N_2$ on a commercial sample of pelletized 4-Å zeolite.

## Carbon Molecular Sieve

### *Pure gas adsorption*

The CMS sample was obtained from Takeda Corporation, Japan. The particles were cylindrical in shape with an effective particle radius (based on external surface area/volume) of 1.7 mm. The material can separate $O_2$ from $N_2$ by a kinetic selectivity (Knoblauch, 1978). The smaller $O_2$ molecules diffuse into the carbon pore-network (internal) faster than the relatively larger $N_2$ molecules because the pore mouth sizes (effective diameter) of the CMS are constricted to be between the molecular diameters of $N_2$ and $O_2$.

Many research groups have studied the diffusion of pure $O_2$ and $N_2$ into CMS produced by different manufacturers using the conventional methods. Table 2 summarizes some of these key works. It may be seen that various mass-transfer mechanisms such as surface barrier at pellet surface (pore mouth restriction), Fickian diffusion into the carbon pore-network (internal), phase exchange reaction, or combinations of two mechanisms have been used to explain the experimental pure gas uptake data.

The CMS was regenerated by heating it to a temperature of 100°C under a flow of dry $N_2$. Figure 3 shows the pure gas adsorption isotherms for $N_2$ on the CMS as measured by the IET at 30 and 50°C. The isotherms were measured by using Eq. 23 and following the mol fractions of $N_2^{30}$ isotope during the exchange process. An example of the experimental data for calculating $n_i^m$ of Figure 3 at a given $P$, $T$ and $y_i$ is shown in Table 3. The open circles in Figure 3 show the pure gas $N_2$ adsorption isotherm at 30°C measured by the conventional VAT in our laboratory. It may be seen that the isotherms measured by the two methods overlap indicating the validity of the assumptions of the IET. The pure gas $N_2$ isotherms are Type I in shape (Brunauer classification).

Figure 4 shows the experimental fractional uptake curves $[f_{N_2^{30}}^*]$ for pure $N_2$ on the CMS as functions of $\sqrt{t}$ at 10, 30, and 50°C. The CMS was initially equilibrated with pure $N_2$ at different pressures so that the overall surface excess of $N_2$ $(n_{N_2}^m)$ for each case was constant at 0.68 mmol/g. The solid lines in Figure 4 are the best fit of the uptake data by the LDF model (Eqs. 34 and 35). They show that the model describes the data extremely well. The $a_{N_2^{30}}^*$ values (Eq. 35) and the isotope mass-transfer coefficients $[k_{N_2^{30}}^*]$ are given in the figure. The ability of the LDF model to describe the uptake data of Figure 4 indicates that the primary mass-transfer resistance for diffusion of $N_2$ into the CMS is controlled by a resistance at the carbon pore mouth.

Figure 5 is a plot of $\ln k_{N_2^{30}}^*$ against reciprocal temperature ($K^{-1}$) for the CMS. The resulting linear plot indicates that

**Table 2. Experimental and Model Studies on Equilibrium and Kinetics of $O_2$ and $N_2$ on CMS**

| Authors | Experimental Method | Mass-Transfer Model | Comments |
|---|---|---|---|
| Knoblauch (1978) | Volumetric (pure gas) | Fickian diffusion | Berbau-Forschung (Germany) CMS |
| Chihara and Suzuki (1979) | Chromatographic (pure gas) | Fickian diffusion | Takeda (Japan) CMS |
| Ruthven, Raghavan and Hassan (1986) | Gravimetric, chromatographic (pure gas) | Fickian diffusion | Bergbau-Forschung (German) CMS |
| LaCava, Koss and Wickens (1989) | Volumetric (pure gas) | Mass action rate process | Experimental CMS |
| Loughlin, Hassan, Fatehi and Zahur (1993) | Gravimetric, volumetric, chromatographic (pure gas, $N_2$ only) | Combined surface barrier-Fickian diffusion within particle | Bergbau-Forschung (Germany) CMS |
| Fitch, Bulow and LaCava (1994) | Gravimetric (pure gas) | Surface barrier, molecular simulation of diffusion in slit shaped pores | Experimental CMS |
| Chen, Yang and Uawithya (1994) | Thermal desorption technique using a differential adsorption bed (pure gas and binary mixtures) | Fickian diffusion | Bergbau-Forschung (Germany) CMS |
| Srinivasan, Auvil and Schork (1995) | Volumetric (pure gas) | Surface barrier, mass action rate process | Source of CMS not disclosed |
| Liu and Ruthven (1996) | Gravimetric (pure gas) | Fickian diffusion | Bergbau-Forschung (Germany) CMS |

the diffusion of $N_2$ through the carbon pore mouth is an activated process. The activation energy ($E^a_{N_2}$) for the process is 7.3 kcal/mol. For comparison, the isosteric heat of adsorption ($q^0_{N_2}$) of $N_2$ on the CMS is 4.0 kcal/mol. It is calculated from the isotherms of Figure 3 using the thermodynamic relationship (Sircar, 1985)

$$\left[q_i^0 = RT^2 \cdot \left(\frac{\delta \ln P}{\delta T}\right)_{n_i^{mo}}\right]. \tag{52}$$

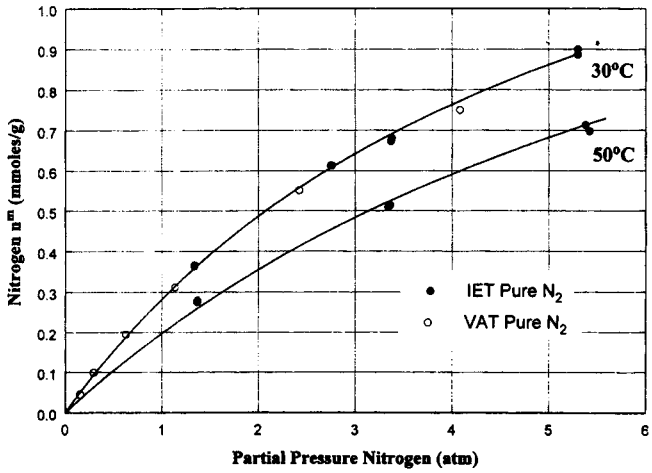


**Figure 3. Pure gas adsorption isotherms for $N_2$ on CMS measured by IET and VAT.**

**Table 3. % Composition for Each Isotope of Pure Nitrogen on CMS***

| | $N_2^{28}$ | $N_2^{29}$ | $N_2^{30}$ |
|---|---|---|---|
| $y^{*o}_{N_2^i}$ | 99.282 | 0.715 | 0.003 |
| $y^{*d}_{N_2^i}$ | 0.142 | 0.112 | 99.746 |
| $y^{**}_{N_2^i}$ | 98.705 | 0.712 | 0.583 |
| $y^{*\infty}_{N_2^i}$ | 98.885 | 0.713 | 0.402 |

*$P$ = 2.75 atm; $T$ = 30°C; $V_s$ = 10.81 cm³/g; $\rho$ = 3.95 cm³/g.

Figure 6 replots the $N_2$ uptake data at 30°C from Figure 4 along with the line (solid) showing the best fit of the data by the LDF model. It also shows a family of uptake lines (dashed) calculated by the CPDF or Fickian Diffusion model (Eqs. 48–50) using the appropriate value of $a_{ij}$ (= 1.45) for the experiment and different values of the parameter ($D^*_{N_2}/a^2$). It is clear from the figure that the Fickian Diffusion model completely fails to describe the uptake of $N_2$ by the CMS.

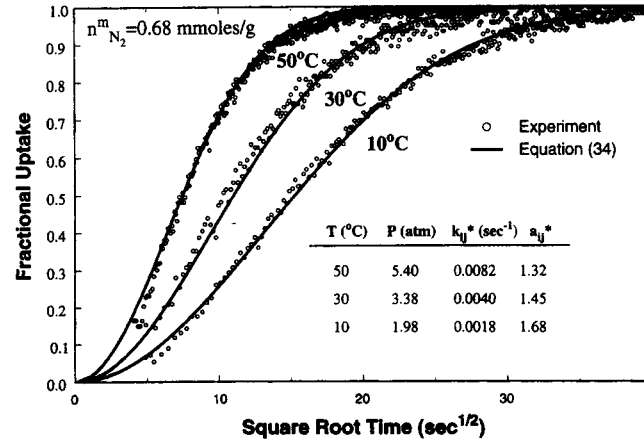


**Figure 4. Uptake curves for adsorption of pure $N_2$ by CMS measured by IET.**

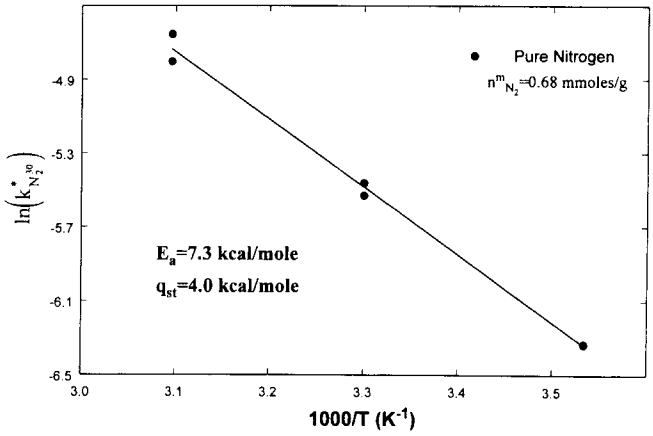


**Figure 5. Arrhenius plot of ($\ln k^*_{N_2}$) against ($1/T$) for adsorption of $N_2$ on CMS.**

### *Binary gas adsorption*

The IET was used to measure the surface excesses for adsorption of $N_2$ (component 1) and $O_2$ (component 2) from their binary mixture ($y_{N_2} = 0.79$, $y_{O_2} = 0.21$) at different total gas pressures and at temperatures of 30 and 50°C. The changes in the mol fractions of $O_2^{36}$ isotope was used to study the $O_2$ adsorption characteristics. Table 4 reports the binary equilibrium adsorption properties. It shows that the thermodynamic selectivity of adsorption of $N_2$ over $O_2$ [$S = n_1^m y_2 / n_2^m y_1$] under the conditions of measurement is equal to unity.

Figure 7 shows the uptakes of $O_2$ and $N_2$ from air ($y_{N_2} = 0.79$) as functions of $\sqrt{t}$ measured at a total gas pressure of 4.21 atmospheres and at a temperature of 30°C. The equilibrium surface excesses of $N_2$ and $O_2$ were respectively, 0.68 and 0.18 mmol/g during the test. The solid lines in Figure 7 represent the best fit of the data by the LDF models (Eqs. 34 and 35). The model parameters are given in the figure. The figure shows that the uptakes of both $O_2$ and $N_2$ can be described by the LDF model extremely well. The transport of both gases into the carbon is controlled by the pore mouth restriction. The isotopic mass-transfer coefficient for $O_2$ uptake by the CMS is, however, 15.5 times faster than that for $N_2$ under the conditions of the experiment, which forms the basis for air separation by the carbon.

**Table 4. Binary Equilibria for Adsorption of Nitrogen and Oxygen on CMS Measured by IET***

| Cond. of Measurement | | Component Surface Excess | | Thermody. Selectivity |
|---|---|---|---|---|
| Pres. (atm) | Temp. (K) | $n^m_{N_2}$ (mmol/g) | $n^m_{O_2}$ (mmol/g) | $n^m_{N_2} \cdot y_{O_2} / n^m_{O_2} \cdot y_{N_2}$ |
| 1.7 | 303 | 0.372 | 0.099 | 1.00 |
| 2.6 | 303 | 0.486 | 0.131 | 0.98 |
| 3.4 | 303 | 0.593 | 0.153 | 1.03 |
| 4.2 | 303 | 0.679 | 0.177 | 1.02 |
| 4.2 | 323 | 0.543 | 0.140 | 1.03 |

*$y_{N_2} = 0.79$; $y_{O_2} = 0.21$.

We also measured the isotopic mass-transfer coefficients for adsorption of $N_2^{30}$ using pure $N_2$ at different total gas pressures and then for adsorption of $N_2^{30}$ and $O_2^{36}$ from binary $N_2 + O_2$ gas mixtures ($y_{N_2} = 0.79$) at different partial pressures of these gases on the CMS at 30°C. Figures 8 and 9, respectively, show the variations in isotopic mass-transfer coefficients of $N_2^{30}$ and $O_2^{36}$ on CMS as functions of the gas-phase partial pressures of these components.

Figure 8 shows that $k^*_{N_2^{30}}$ linearly increases with gas-phase $N_2$ partial pressure in the range of the data. The very interesting result is that the presence of $O_2$ in the gas phase does not appreciably change the isotopic mass-transfer coefficient for the $N_2^{30}$. Figure 9 shows that $k^*_{O_2^{36}}$ also increases linearly with increasing gas-phase partial pressure of $O_2$ in pressure of $N_2$ ($y_{N_2} = 0.79$). The sensitivity of the $k^*_{O_2^{36}}$ to $P_{O_2}$ plot is, however, much less than the sensitivity of $k^*_{N_2^{30}}$ to $P_{N_2}$. The reason for this observed behavior is not clear.

Table 5 shows a compilation of several published experimental data on time constants for transport of pure $N_2$ and $O_2$ into various CMS samples. The time constants are reported as [$D/a^2$] where the data were analyzed by the Fickian diffusion model, and as [$k$] where the data were analyzed

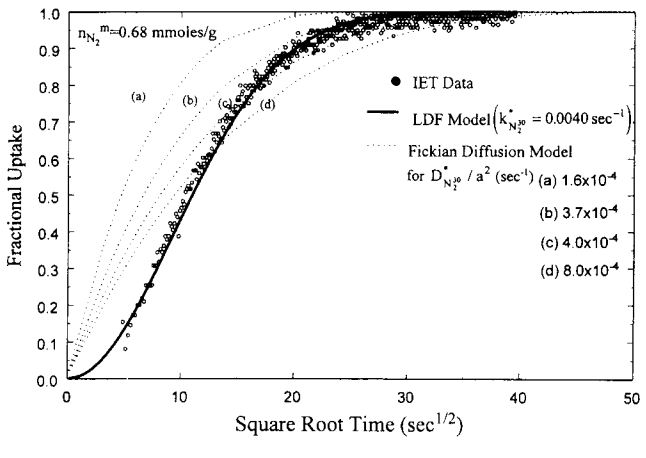


**Figure 6. Comparison of pure $N_2$ uptake data on CMS by LDF and Fickian diffusion models at 30°C.**

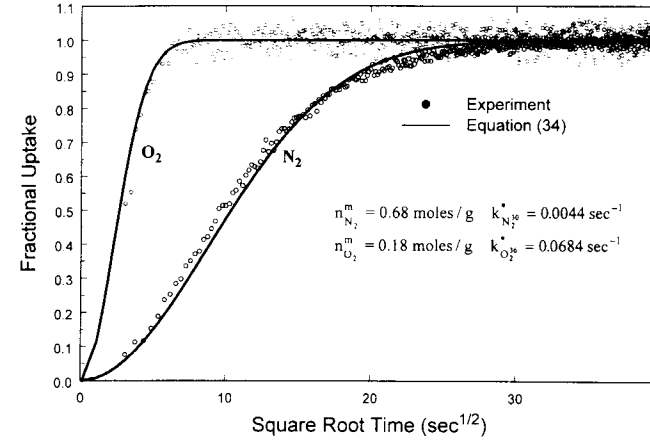


**Figure 7. Comparison of uptake curves for adsorption of $O_2$ and $N_2$ on CMS from air measured by IET at 30°C with LDF model.**

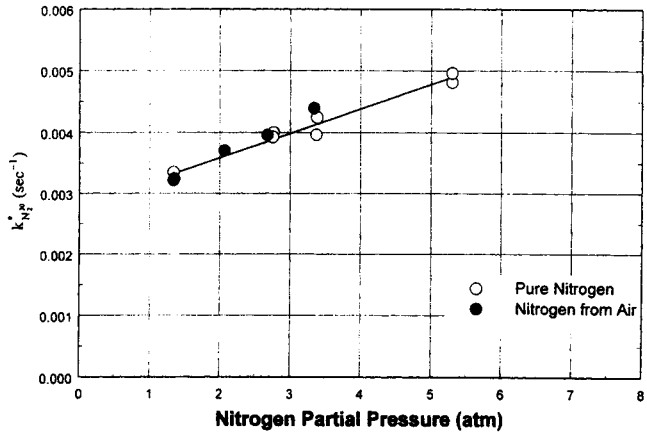


**Figure 8. Partial pressure dependence of isotopic mass-transfer coefficients for $N_2$ adsorption on CMS at 30°C.**

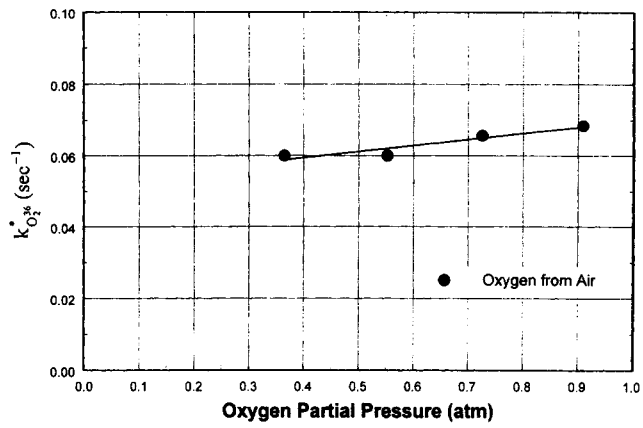


**Figure 9. Partial pressure dependence of isotopic mass-transfer coefficients for $O_2$ adsorption from air on CMS at 30°C.**

by a surface barrier resistance model. The values of the CMS particle radius $a$ are given when available. The table also shows the idealized kinetic selectivity of the CMS for $O_2$ over $N_2$ ($D_{O_2}/D_{N_2}$ or $k_{O_2}/k_{N_2}$) assuming that the transport properties of these gases do not change in presence of each other. It may be seen that the reported transport properties for $N_2$ and $O_2$ into CMS samples of different sources (or even same source) differ substantially (Table 5).

The mass-transfer coefficients for self-diffusion of $N_2$ and $O_2$ from their binary mixtures into the Takeda CMS sample at two different total gas pressures (measured by the IET of present work) are also reported in Table 5. They show that the transport coefficient for self-diffusion of these gases from air are much higher than those reported in the literature for other CMS samples. The kinetic selectivities of adsorption of $O_2$ over $N_2$ on the Takeda CMS sample are lower than those for the other CMS samples, but they are of comparable magnitude. The self-diffusion transport coefficients for $O_2$ and $N_2$ from air increased with increasing total gas pressure on the Takeda CMS sample, but the kinetic selectivity of $O_2$ over $N_2$ decreased. The activation energy for self-diffusion of pure $N_2$ on the Takeda CMS sample was comparable with those for other samples.

## 4-Å Zeolite

### *Pure gas adsorption*

The 4-Å zeolite beads ($a = 1.0$ mm) used in our IET were obtained from UOP, U.S.A. They were regenerated by heating to 400°C under vacuum for 12 h. Figure 10 shows the equilibrium adsorption isotherms of pure $N_2$ on 4-Å zeolite at $-20$°C and 10°C measured by IET. Again, $N_2^{30}$ was used in these tests as the probe isotope. The isotherms are Type I in shape.

Figure 11 shows an example of the uptake of $N_2^{30}$ as a function of $\sqrt{t}$ by the zeolite at $-20$°C. The solid line in Figure 11 is the best fit of the data by the CPDF or Fickian diffusion model (Eqs. 48–50). The model parameters [$D^*_{N_2^{30}}/a^2$ and $\alpha_{ij}$] are given in the figure. The Fickian diffusion model describes the data extremely well. The dashed lines in Figure 11 represent a family of plots of fractional uptake against $\sqrt{t}$ calculated using the LDF model with different values of $k^*_{N_2}$.

**Table 5. Literature Values of Transport Coefficients and Activation Energies for Adsorption of Pure Nitrogen and Oxygen on Various CMS**

| Authors | Particle Radius (mm) | Conditions of Measurement: Pres. (atm) | Conditions of Measurement: Temp. (K) | Time Constants ($\times 10^4$): $(D/a^2)$, $s^{-1}$: $N_2$ | Time Constants ($\times 10^4$): $(D/a^2)$, $s^{-1}$: $O_2$ | Time Constants ($\times 10^4$): $k$, $s^{-1}$: $N_2$ | Time Constants ($\times 10^4$): $k$, $s^{-1}$: $O_2$ | Kinetic Selectivity $(D_{O_2}/D_{N_2})$ or $(k_{O_2}/k_{N_2})$ | Activation Energy (kcal/mol): $N_2$ | Activation Energy (kcal/mol): $O_2$ |
|---|---|---|---|---|---|---|---|---|---|---|
| Knoblauch (1978) | | — | — | 7.0 | 170.0 | — | — | 24.2 | — | — |
| Ruthven et al. (1986) | 2.5 | 0.23–0.88 | 303 | 1.2 | 37.0 | — | — | 30.8 | 6.5 | — |
| Lui and Ruthven (1996) | — | 0.76–0.94 | 273 | 0.035 | 2.4 | — | — | 68.6 | — | — |
| Loughlin et al. (1993) | — | — | 298 | — | — | 0.24 | — | — | 8.1 | — |
| Chen et al. (1994) | 1.9 | $P \to 0$ | 300 | 0.095 | 3.5 | — | — | 36.8 | — | — |
| Dominguez et al. (1988) | — | — | 298 | — | — | 1.9 | 82.5 | 43.4 | — | — |
| This Work* | 1.7 | 1.0 | 303 | — | — | 32.0 | 600.0 | 21.9 | 7.3 | |
| | | 4.2 | 303 | | | 44.0 | 684.0 | 15.5 | | |

*Self-diffusion of $N_2$ and $O_2$ from synthetic air ($y_{N_2} = 0.79$, $y_{O_2} = 0.21$).

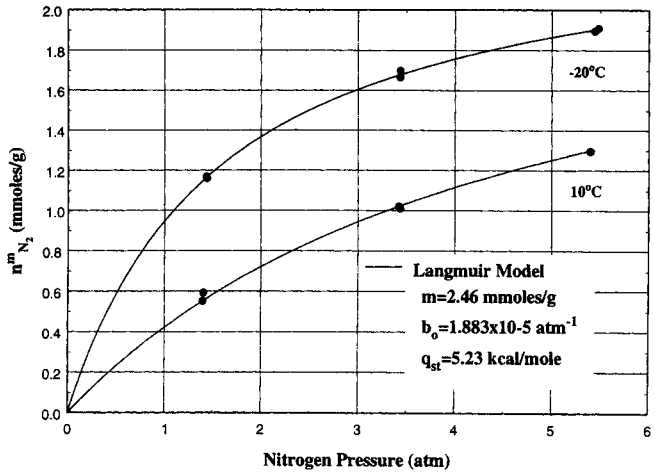


**Figure 10. Pure gas adsorption isotherms for $N_2$ on 4-Å zeolite measured by IET.**

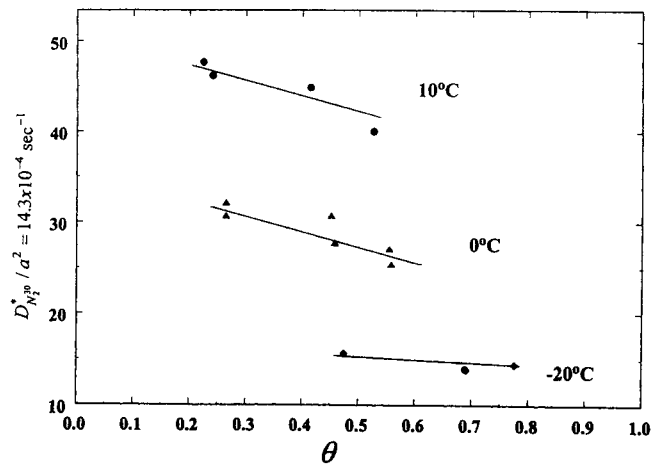


**Figure 12. Adsorbate loading (surface excess) dependence on self-diffusion coefficient for $N_2$ adsorption on 4-Å zeolite.**

They show that the diffusion of $N_2$ into the 4-Å zeolite cannot be described by the LDF model.

We also measured the self-diffusivity of $N_2$ into 4-Å zeolites at different equilibrium surface excess values ($n^m_{N_2}$) of the adsorbate and at three different temperatures. Figure 12 shows the results where $[D^*_{N_2^{30}}/a^2]$ values are plotted as functions of fractional coverages ($\theta$) of $N_2$. The isotherms of Figure 10 can be described by the Langmuir model with a $N_2$ saturation capacity (m) of 2.46 mmol/g. The other Langmuirian parameters are given in the figure. The fractional coverage is defined by $[\theta = n^m_{N_2}/m]$. It may be seen from Figure 12 that the self-diffusivities of $N_2$ in 4-Å zeolite decrease with increasing adsorbate loadings (surface excess). This behavior is opposite to that observed for diffusion of $N_2^{30}$ through the pore mouth of CMS. There is no clear mechanistic explanation for this behavior.

The data of Figure 12 are replotted as $\ln[D^*_{N_2^{30}}/a^2]$ against reciprocal temperature ($K^{-1}$) (at a constant value of $n^m_{N_2}$) in Figure 13. The linearity of the plot indicates that $N_2$ diffusion in 4-Å zeolite is an activated process with an activation energy ($E^a_{N_2}$) of 4.4 kcal/mol. The isosteric heat of adsorption of $N_2$ on 4-Å zeolite is 5.2 kcal/mol as calculated from the isotherms of Figure 10 using Eq. 52.

Table 6 reports several values of time constants ($D/a^2$) for Fickian diffusion of pure $N_2$ into 4-Å zeolite crystals from published literature. The data were measured using different crystal radii under different conditions of experiments. It may be seen that the published $N_2$ diffusivity (transport) values differ by a large range. The time constant for self-diffusion of pure $N_2$ into the pelletized 4-Å zeolite sample of this work is comparable to those measured on several samples of 4-Å crystals. The approximate relationship ($k = 15D/a^2$) may be used to carry out the comparison (Ruthven, 1984). That indicates that the primary resistance for diffusion of $N_2$ into the 4-Å pellet of this work was within the zeolite crystals. The activation energy for self-diffusion of $N_2$ into the pelletized 4-Å zeolite measured by IET was comparable with those measured for transport diffusion of $N_2$ into 4-Å crystals.

## External Gas Film Transport Resistances

Assuming that the gas-phase external film mass-transfer resistance for the $j$th isotope of component $i$ is in series with

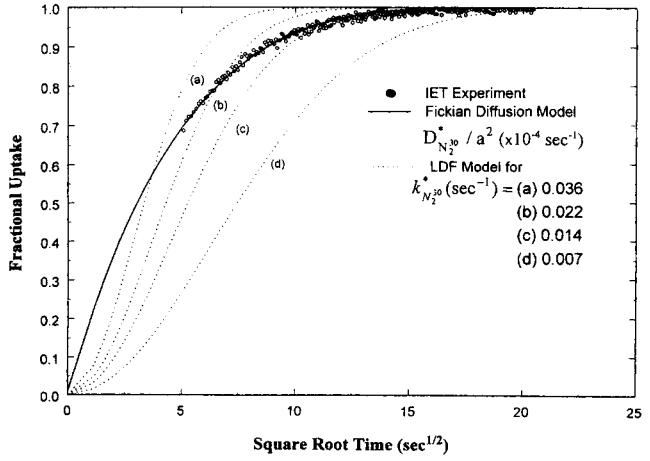


**Figure 11. Uptake curve for adsorption of pure $N_2$ by 4-Å zeolite measured by IET at -20°C.**

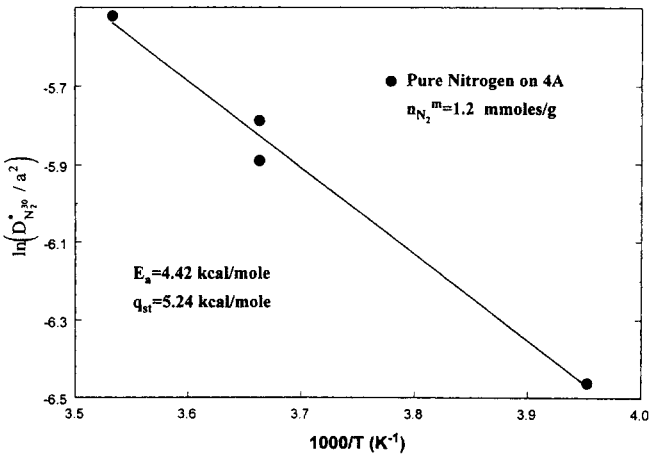


**Figure 13. Arrhenius plot of $[\ln(D^*_{N_2}/a^2)]$ against $(1/T)$ for adsorption of $N_2$ on 4-Å zeolite.**

**Table 6. Literature Values of Fickian Diffusivities and Activation Energies for Transport of Nitrogen in 4-Å Zeolite**

| Authors | Crystal Radius ($\mu$m) | Conditions of Measurement: Pres. (atm) | Conditions of Measurement: Temp. (K) | Time Constant $(D/a^2)$ ($s^{-1}$) | Activation Energy (kcal/mol) |
|---|---|---|---|---|---|
| Habgood (1958) | 0.25 | $P \to 0$ | 300 | $39.9 \times 10^{-4}$ | 4.1 |
| Haq and Ruthven (1986) | 2.5 | $P \to 0$ | 298 | $29.4 \times 10^{-4}$ | — |
| Cartigny et al. (1994) | 1.9 | < 0.20 | 273 | $24.9 \times 10^{-4}$ | — |
| Van der Voorde et al. (1990) | 50.0 | < 0.26 | 298 | $0.048 \times 10^{-4}$ | 5.3 |
| This work* | Pellet (radius 1.0 = mm) | 1.39 | 283 | $40 \times 10^{-4}$ | 4.4 |

*Self-diffusion of pure $N_2$ in 4-Å zeolite pellet.

a lumped mass-transfer resistance within the adsorbent particle, one can easily show that

$$\frac{1}{k_{ij}^*} = \frac{1}{k_{ij}^{a*}} + \frac{K_i}{k_{ij}^{*g}} \tag{53}$$

where $k_{ij}^*$ ($s^{-1}$) is the measured mass-transfer coefficient for the $j$th isotope of component $i$ by the IET using the LDF or CPDF models [$k_{ij}^* \simeq 15D_{ij}^*/a^2$]. The parameter $K_i$ (dimensionless) is given by [$\rho_p n_i^m/\rho y_i$]. The variable $k_{ij}^{*a}$ ($s^{-1}$) is the mass-transfer coefficient for $j$th isotope of component $i$ for the lumped internal resistances within the adsorbent particle. The variable $k_{ij}^{*g}$ is the external gas film mass-transfer coefficient for the $j$th isotope of component $i$ over a particle of radius $a$ (Satterfield, 1970).

Equation 53 is derived by replacing the actual adsorption system of IET with the previously described model system (Crank, 1956) consisting of a spherical adsorbed phase of radius $a$ (volume $V_a$) and a gas phase of volume $V_b$ ($= V$) where the gas is circulated over the adsorbent with a flow rate of $G_M$. According to this model, it can be shown that the average concentration of the $j$th isotope of component $i$ in the adsorbed phase [$\bar{C}_{ij}^*(t)$] at time $t$ is equal to [$\rho_P n_i^{*m}(t)$], where $n_i^{*m}(t)$ is the corresponding surface excess in the IET experiment.

We estimated the relative values of the external gas film transport resistances [$K_i/k_{ij}^{*g}$] for each of the IET runs. It was found that the term [$K_i/k_{ij}^{*g}$] was less than 3.0% of the term [$1/k_{ij}^*$] in each case. Thus, the external gas film resistances were not important for self-diffusion of the isotopes of $N_2$ and $O_2$ into the pellets of CMS and 4-Å zeolite evaluated in this work.

## Summary

The isotope exchange technique (IET) is demonstrated to be a powerful tool for simultaneous measurement of multicomponent gas adsorption equilibria (surface excess of each component of the mixture at a given $P$, $T$ and $y_i$) and kinetics (self-diffusion or mass-transfer coefficients of each component of the mixture at a given $n_i^m$ and $T$) in a single experiment. The key advantages of the method include (a) complete control over the state of adsorption equilibrium on the adsorbent which remains undisturbed during the experiment, (b) truly isothermal uptake (loss) of the adsorbates, and (c) relative ease of experimental replicability.

The IET was used to measure the equilibria and kinetics for adsorption of $N_2$ as a pure gas and in binary mixtures with $O_2$ on a commercial carbon molecular sieve (CMS) at different temperatures. It was shown that the uptakes of $N_2$ (pure and in mixture of $O_2$) and $O_2$ (in mixture with $N_2$) by the CMS could be described by the linear driving force model. This indicated that the isotopic mass-transfer resistances (self-diffusivities) for these gases into the CMS internal pore-network were controlled by the constrictions at the pore mouths of the CMS. The diffusion was an activated process and the isotopic mass-transfer coefficients for both $N_2$ and $O_2$ increased linearly with increasing partial pressures of these components in the gas phase. The effects of gas-phase $N_2$ partial pressures on the transfer coefficients for $N_2$ were more pronounced than the effects of gas-phase $O_2$ partial pressures on the transfer coefficients for $O_2$. The transfer coefficients for $N_2$ at a given gas-phase $N_2$ partial pressure and temperature were practically the same for adsorption of $N_2$ as a pure gas or that from air. The equilibrium selectivity for adsorption of $O_2$ over $N_2$ on CMS was unity over a large range of pressure and temperature. The self-diffusivities of both $N_2$ and $O_2$ increased with increasing total gas pressure but the kinetic selectivity of $O_2$ over $N_2$ decreased.

The IET was also used to measure the adsorption equilibria and kinetics of pure $N_2$ on 4-Å zeolite at different temperatures. It was shown that the self-diffusion of $N_2$ on the zeolite could be described by the Fickian diffusion model. The self-diffusivities of $N_2$ decreased with increasing $N_2$ adsorbate loading (surface excess) and the diffusion process was activated.

## Acknowledgments

The authors are grateful to Judith M. Shabrach for carrying out the experimental measurements, Dr. Timothy C. Golden for measuring the pure $N_2$ adsorption isotherm on CMS by VAT, and Dr. Kenneth J. Anselmo for assisting with data analysis.

## Notation

$\bar{C}_{ij}^*$ = total average concentration of $j$th isotope of component $i$ in adsorbent particle
$D_{jm}$ = diffusivity of $j$th isotope of component $i$ at $P$, $T$, $y_i$
$k_{ij}^{*a}$ = internal mass-transfer coefficient of $j$th isotope of component $i$
$k_{ij}^{*g}$ = external film mass-transfer coefficient of $j$th isotope of component $i$
$m$ = Langmuirian saturation capacity
$V$ = total volume of IET apparatus ($V_m + V_d$)
$V_d$ = volume of dosing loop of IET apparatus
$V_m$ = helium volume of main loop of IET apparatus
$y_{ij}^{*0}$ = gas-phase mol fraction of $j$th isotope (dilute) of component $i$ in the saturating gas
$y_{ij}^{**}$ = gas-phase mol fraction of $j$th isotope (dilute) of component $i$ after mixing between dosing and main loop gas at $t = 0$
$y_{ij}^{*\infty}$ = gas-phase mol fraction of $j$th isotope (dilute) of component $i$ at $t = \infty$
$(e)$ = property at equilibrium
$(0)$ = property at $t = 0$
$(\infty)$ = property at $t \to \infty$

### *Superscripts*

$0$ = property at $t = 0$
$\infty$ = property at $t \to \infty$
$**$ = mixed gas property after contact between dosing and main loops of IET apparatus ($t = 0$)
$d$ = gas-phase property of dosing loop
$s$ = gas-phase property at start of IET experiment
$m$ = experimentally measured surface excess
$R$ = all isotopes species other than the dilute $j$th isotope
$\overline{\ }$ = average concentration in adsorbent particle

### *Subscripts*

$ij$ = $j$th isotope of $i$th component
$i$ = $i$th species

## Literature Cited


Barrer, R. M., *Intracrystalline Diffusion*, Adv. in Chemistry Ser., **102**, 1, *R. F. Gould, ed., ACS* (1971).

Basmadjian, J. D., "Adsorption Equilibriums of $H_2$, $D_2$ and Their Mixtures," *Can. J. Chem.*, **38**, 141 (1960).

Brandani, S., J. R. Hufton, and D. M. Ruthven, "Self-Diffusion of Propane and Propylene in 5Å and 13X Zeolite Studied by the Tracer ZLC Method," *Zeolites*, **15**, 624 (1995).

Breck, D. W., *Zeolite Molecular Sieves*, R. E. Krieger Publishing, Malabar, FL (1984).

Callen, H. B., *Thermodynamics*, Wiley, New York (1965).

Cartigny, J., J. Giermanska-Kahn, and E. Cohen DeLara, "Frequency Response Method in Study of Methane Diffusion in the Cation Exchanged Zeolites A," *Zeolites*, **14**, 576 (1994).

Chen, Y. D., R. T. Yang, and P. Uawithya, "Diffusion of Oxygen, Nitrogen and Their Mixtures in Carbon Molecular Sieves," *AIChE J.*, **40**, 577 (1994).

Chihara, K., and M. Suzuki, "Control of Micropore Diffusivities of Molecular Sieve Carbon by Deposition of Hydrocarbons," *Carbon*, **17**, 339 (1979).

Crank, J., *Mathematics of Diffusion*, Oxford University Press, London (1956).

Dominguez, J. A., D. Psaras, and A. I. Lacava, "Langmuir Kinetics as an Accurate Simulation of Rate of Adsorption of $O_2$ and $N_2$ Mixtures on non Fickian Carbon Molecular Sieves," *AIChE Symp. Ser.*, **84**, 73 (1988).

Dunne, J., M. B. Rao, S. Sircar, R. J. Gorte, and A. L. Myers, "Calorimetric Heats of Adsorption and Adsorption Isotherms: Mixtures of $CH_4$ and $C_2H_6$ in Silicalite and Mixtures of $CO_2$ and $C_2H_6$ in NaX," *Langmuir*, in press (1997).

Dutel, J. F., M. Seibold, and P. Gelin, "Diffusion of Molecules in Zeolites Studied by a Transient Isotopic Method," *Adsorption Processes for Gas Separation*, F. Meurier and M. D. Levan, eds., Nancy, France, p. 95 (1991).

Forste, C., J. Karger, and H. Pfeiffer, "Self-Diffusion Studies by NMR Tracer Uptake Measurements," *Zeolites: Facts, Figures, Future*, P. A. Jacobs and R. A. van Santen, eds., Elsevier Science, Amsterdam, p. 907 (1989).

Goddard, M., and D. M. Ruthven, "Sorption and Diffusion of $C_8$ Aromatic Hydrocarbons in Faujasite Type Zeolites: Self-Diffusivities by Tracer Exchange," *Zeolites*, **6**, 445 (1986).

Habgood, H. W., "The Kinetics of Molecular Sieve Action, Sorption of Nitrogen-Methane Mixtures by Linde Molecular Sieve 4A," *Can. J. Chem. Eng.*, **36**, 1384 (1958).

Haq, N., and D. M. Ruthven, "Chromatographic Study of Sorption and Diffusion in 4A Zeolite," *J. Colloid and Interf. Sci.*, **112**, 154 (1986).

Hartzog, D. G., and S. Sircar, "Sensitivity of PSA Process Performance to Input Variables," *Adsorption*, **1**, 133 (1995).

Helfferich, F., and D. L. Peterson, "Accurate Chromatographic Method for Sorption Isotherms and Phase Equilibria," *Science*, **42**, 661 (1963).

Hufton, J. R., and R. P. Danner, "Gas-Solid Diffusion and Equilibrium Parameters by Tracer-Pulse Chromatography," *Chem. Eng. Sci.*, **46**, 2079 (1991).

Hyun, S. H., and R. P. Danner, "Adsorption Equilibrium Constants and Intraparticle Diffusivities in Molecular Sieves by Tracer-Pulse Chromatography," *AIChE J.*, **31**, 1077 (1985).

Karger, J., and D. M. Ruthven, *Diffusion in Zeolites*, Wiley-Interscience, New York (1992).

Knoblauch, K., "Pressure Swing Adsorption Geared for Small Volume Users," *Chem. Eng.*, **85**, 87 (1978).

Kumar, R., and S. Sircar, "Skin Resistance for Adsorbate Mass Transfer into Extruded Adsorbent Pellets," *Chem. Eng. Sci.*, **41**, 2215 (1986).

Lacava, A. I., V. A. Koss, and D. Wickens, "Non-Fickian Adsorption Rate Behavior of Some Carbon Molecular Sieves," *Gas Sep. Purif.*, **3**, 180 (1989).

Liu, H., and D. M. Ruthven, "Diffusion in Carbon Molecular Sieves," *Proc. 5th Int. Conf. Fund. Adsorp.*, M. D. LaVan, ed., Kluwer Press, Boston, p. 529 (1996).

Loughlin, R. F., M. M. Hassan, A. I. Fatehi, and M. Zahur, "Rate and Equilibrium Sorption Parameters for Nitrogen and Methane on Carbon Molecular Sieve," *Gas Sep. Purif.*, **7**, 264 (1993).

Morikawa, Y., and A. Ozaki, "Displacement of Adsorbed Nitrogen Accompanied by Isotopic Mixing Over Unpromoted Iron," *J. Catal.*, **12**, 145 (1968).

Nanba, M., Y. Oishi, and K. Ando, "Analysis of Precision in Determination of Diffusion Coefficients by the Isotope Exchange Technique," *Memoirs of Faculty of Engineering*, Kyushu Univ., **42**, 245 (1982).

Peterson, D. L., F. Helfferich, and R. J. Carr, "Measurement of Phase Equilibria at High Pressures by Tracer-Pulse Chromatography," *AIChE J.*, **12**, 903 (1966).

Prausnitz, J. M., *Molecular Thermodynamics of Fluid Phase Equilibria*, Prentice Hall, Englewood Cliffs, NJ (1969).

Quig, A., and L. V. C. Rees, "Self-Diffusion of *n*-Alkanes in Type A Zeolite," *J. Chem. Soc. Faraday Trans. I*, **72**, 771 (1976).

Ross, S., and J. P. Olivier, *On Physical Adsorption*, Interscience Publishers, New York (1964).

Ruthven, D. M., *Principles of Adsorption and Adsorption Processes*, Wiley, New York (1984).

Ruthven, D. M., N. S. Raghavan, and M. M. Hassan, "Adsorption and Diffusion of Nitrogen and Oxygen in a Carbon Molecular Sieve," *Chem. Eng. Sci.*, **41**, 1325 (1986).

Satterfield, C. N., *Mass Transfer in Heterogeneous Catalysis*, M.I.T. Press, Cambridge, MA (1970).

Sircar, S., "Data Representation for Binary and Multicomponent Gas Adsorption Equilibria," *Adsorption*, **2**, 327 (1996).

Sircar, S., "Excess Properties and Thermodynamics of Multicomponent Gas Adsorption," *J. Chem. Soc. Faraday Trans. I*, **81**, 1527 (1985).

Sircar, S., "Linear Driving Force Model for Non-Isothermal Gas Adsorption Kinetics," *J. Chem. Soc. Faraday Trans. I*, **79**, 2085 (1983).

Sircar, S., "Non-Isothermal Differential Adsorption Kinetics for Binary Gas Mixture," *I&EC Res.*, **33**, 1585 (1994).

Sircar, S., "Pressure Swing Adsorption: Research Needs by Industry," *Fundamentals of Adsorption*, A. B. Mersmann and S. E. Scholl, eds., p. 815 (1991).

Srinivasan, R., S. R. Auvil, and J. M. Schork, "Mass Transfer in Carbon Molecular Sieves: An Interpretation of Langmuir Kinetics," *Chem. Eng. J.*, **57**, 137 (1995).

Takeuchi, Y., and K. Kawazoe, "Diffusion of Carbon Dioxide Within Molecular Sieve Particles," *J. Chem. Eng. Japan*, **9**, 46 (1976).

Valenzuela, D. P., and A. L. Myers, "Gas Adsorption Equilibria," *Sep. Purif. Methods*, **13**, 153 (1984).

Valenzuela, D. P., and A. L. Myers, *Adsorption Equilibrium Data Book*, Prentice Hall, Englewood Cliffs, NJ (1989).

Van der Voorde, M., Y. Tavernier, J. Martens, H. Verelist, P. Jacobs, and G. Baron, "Chromatographic Study of Adsorption Equilibria and Micropore Diffusion Constants of Permanent Gases in Synthetic Zeolites of LTA, FAU and SOD Type," *Gas Separation Technology*, E. F. Vansant and R. Dewolfs, eds., Elsevier, Amsterdam, p. 303 (1990).


*Manuscript received Jan. 21, 1997, and revision received May 12, 1997.*